JOURNAL OF THERMOPHYSICS AND HEAT TRANSFER
Vol. 11, No. 3, July–September 1997

Characteristics of Ice Slurry Containing Antifreeze Protein for Ice Storage Applications

Svein Grandum*
University of Tsukuba, Tsukuba, Ibaraki 305, Japan
Akira Yabe,† Makoto Tanaka,‡ and Fumio Takemura§
Mechanical Engineering Laboratory, Tsukuba, Ibaraki 305, Japan
and
Kazuya Nakagomi¶
Toyama Medical and Pharmaceutical University, Toyama 930-01, Japan

For the development of flowable ice for storage and long distance transportation purposes, that is resistant to recrystallization and contains defined crystal structures, the characteristics of an ice slurry generated from an antifreeze protein solution have been examined. Three methods for obtaining the antifreeze protein are described. In crystal growth studies it has been shown that controlling the supercooling is important to generate the desired needle-type crystals, coming from an effective adsorption of antifreeze proteins to the ice surface. The ice slurry's thermal storage ability is found using a differential scanning calorimeter. Furthermore, the slurry's flowability is examined using both a capillary tube viscometer and a test loop, the latter is used for comparison of the pressure drop with liquid pure water as well as for the visualization of the slurry flow. For an ice content of 30%, the pressure drop in a 6-mm-i.d. tube at 1 m/s flow is found to be twice the value for liquid pure water.

Nomenclature

D = i.d. capillary tube, m
L = length of capillary tube, m
V = average linear velocity in the tube length direction, m/s
x = position of the capillary tube slurry column from the top, m
ΔP_f = frictional pressure drop, Pa
μ_e = effective viscosity, Pa s

Introduction

ICE slurry is a promising working fluid for low-temperature energy storage systems. A flow of ice crystals has a large cooling capacity as a result of the involvement of latent heat. Compared to conventional systems utilizing the sensible heat, slurry systems will necessarily give a lower mass flow rate, reducing the system dimensions. Several dynamic ice formation techniques have thus been developed.[1–3] Methods of dynamic ice formation of pure water can be categorized as follows: thin film ice on a cooled metal surface, ice formation in the depressurized box, dynamic ice formation by the use of supercooled water, ice formation by the use of direct contact with refrigerant, and ice formation by the use of a small bubble of air.

Furthermore, ice slurry systems utilizing clathrates, polymers, and organic liquids have been developed. However, there are still problems related to the recrystallization of ice crystals for realizing long-term storage and long-distance transportation. To find improvements for this, a method for the creation of ice crystals resistant to recrystallization has been proposed and researched by the use of an antifreeze protein (AFP) solution.

Fish living in subzero ambient conditions survive by depressing the freezing point of blood by the presence of freeze-inhibiting proteins.[4,5] These proteins are mainly known as AFPs and antifreeze glycoproteins (AFGPs). Different from dissolved substances like salt, sugar, glycerol, etc., that lower the freezing point colligatively, these proteins lower the freezing point of blood in a noncolligative manner.[5]

AFPs and AFGPs are quite different in molecular structure; however, the reported effects on the antifreeze activity as well as crystal growth are similar.[5–7] These proteins are adsorbing to the ice crystal surface and disturb the crystal growth.[7] However, mechanisms for the interaction between the α-helical AFP (which is to be further discussed here) and the ice crystal lattice have yet to be cleared. Knight et al.[7] indicated that there are hydrogen bonds between systematically repeated hydrophilic (polar) amino acids located on one side of the helix and oxygen atoms in the ice crystal grid. Because of the hydrophobic (nonpolar) amino acids located on the opposite side of the helical AFP molecule, further crystal growth is inhibited in that direction, creating individually existing needle-type crystals. The ability for these crystals to prevent recrystallization is important for improving the low-temperature energy storage and distribution performance in district cooling systems and in buildings.

So far various applications utilizing AFPs have been proposed. The strong ability of inhibiting recrystallization even at low concentrations[8] makes it promising for food preservation. Furthermore, AFPs have the potential for avoiding the creation of hydrate plugs in petroleum multiphase flow, as well as the potential to be used for body tissue preservation in the medical field.

To examine the potential for low-temperature storage system applications based on ice slurry from an AFP solution, in this

Received Oct. 8, 1996; revision received Feb. 21, 1997; accepted for publication Feb. 25, 1997.

*Graduate Student, Institute of Engineering Mechanics, 1-1-1 Tennodai.
†Associate Professor, Head of Fluid Engineering Division, Ministry of International Trade and Industry, Energy Engineering Department, Mechanical Engineering Laboratory, 1-2 Namiki.
‡Senior Research Scientist, Ministry of International Trade and Industry, Energy Engineering Department, 1-2 Namiki.
§Research Scientist, Ministry of International Trade and Industry, Energy Engineering Department, 1-2 Namiki.
¶Associate Professor, Faculty of Pharmaceutical Sciences, 2630 Sugitani.

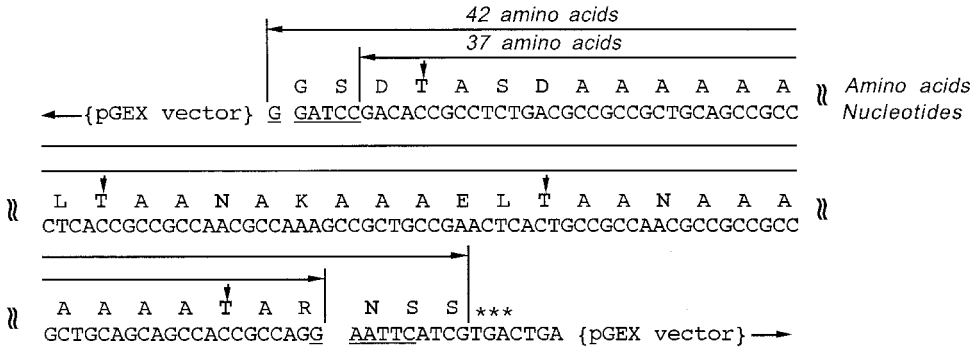

Fig. 1 Amino acid and DNA sequences of molecularly–biologically synthesized AFP (42 amino acids) based on the amino acid sequence of AFP found in Winter Flounder (37 amino acids). Amino acids: G, glycine; S, serine; D, aspartic acid; T, threonine; A, alanine; L, leucine; N, asparagine; K, lysine; E, glutamic acid; and R, arginine.

paper we are reporting the experimental results of storage ability and flowability. The temperature and stored enthalpy relation is shown, representing the low-temperature storage characteristics. Furthermore, the flowability has been examined by use of a viscometer as well as by a laboratory scale loop.

Materials and Methods

Obtaining AFP

In this research one of the low molecular weight AFPs (3200 Dalton), found in the Antarctic Ocean fish, Winter Flounder (*Pleuronectes americanus*), has been utilized. The length of this α-helical AFP is approximately 50 Å and the diameter is 10 Å.[6,7] Its repeated polar amino acids (threonine) are located at the same side, aligned slightly skew compared to the helix axis. This molecule has a relatively high content (~60%) of the nonpolar alanine (A), mainly located on the opposite side of the helix.[6] The amino acid composition is shown in Fig. 1.

AFP, for the purpose of creating ice slurry can, in principle, be obtained in three different ways where our studies have been utilizing AFP based on all three methods.

Chemically Synthesized

Based on the composition information of the 37-amino acid AFP (Fig. 1) from the Winter Flounder,[9] the chemically synthesized protein was ordered as a reference to the AFP made by the following two methods. For higher molecular weight proteins such a synthesis will include several steps and become expensive when a larger amount is synthesized. Analysis of the sample by reversed-phase high-performance liquid chromatography (HPLC) showed a purity of 96%.

Synthesized in Bacterial Cells

This method, synthesizing AFP molecularly–biologically in bacterial cells by the use of a recombinant protein-expressing plasmid vector, has utilized DNA sequencing information in coding the amino acid sequence of AFP. Contrary to the chemical synthesis, this method has the ability to synthesize even the higher molecular weight proteins as well as produce a large amount of protein by increasing the scale of bacterial cultivation. Utilizing this method, the 42-amino acid AFP was synthesized as follows (Fig. 1): double-stranded nucleotides coding for the amino acid sequence of AFP[10] were chemically synthesized. These nucleotides have restriction enzyme-cutting sites, BamH1 site (GGATCC) and EcoR1 site (GAATTC) at each terminal to connect to the protein-expressing plasmid, pGEX2T. The plasmid vector pGEX(AFP) was constructed by inducing those nucleotides to the BamH1 and EcoR1 site of the pGEX2T. The extra five amino acids were added to the 37-amino acid AFP, two at one end (GS) of the protein and three at the other (NSS) to construct the plasmid vector. However, this was thought to have little effect on the antifreeze activity caused by the maintenance of the structure. *Escherichia coli* DH5α bacteria were cultivated by an ordinary way after being transformed with the pGEX(AFP). AFP was then synthesized as glutathione-S-transferase (GST) fusion protein in bacterial cells after adding isopropyl-1-thio-β-D-galactoside (IPTG) as an inducer. AFP was applied to the glutathione-sepharose 4B affinity column and eluted after thrombin digestion at the connecting site with GST in the column. Finally, purification was performed through a Sep-Pak C18 cartridge. The purity by HPLC analysis was found to be the same as the chemically synthesized AFP. Using this method, 1.5-mg AFP could be obtained from 1 l of bacterial culture broth. This method was used to produce AFP for the ice slurry experiments, except the loop experiments.

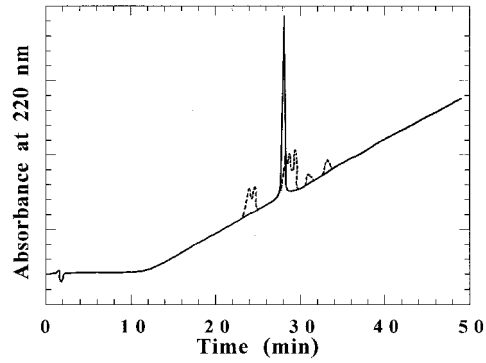

Fig. 2 Comparison of the chemically synthesized AFP (continuous line) with the purified AFP from fish (discontinuous line) by reversed-phase HPLC.

Purified from the Blood of Fish

AFP purified from fish blood[11] is normally composed by several AFP molecules, which have similar shapes and properties.[12] AFP from Winter Flounder, AFP I, was analyzed using reversed-phase HPLC. On the chart, several peaks close to the peak of the chemically synthesized AFP were found, as illustrated in Fig. 2. This indicates a probable similarity in the molecular structure. AFP purified from fish blood is less expensive than AFP obtained from the two previously mentioned methods. In the ice slurry loop experiments, where a large amount of protein was required, this type of AFP was utilized.

The chemically synthesized AFP as well as the AFP purified from fish blood was delivered in dried condition. To dissolve these properly, NaOH was added, since a basic solution turned out to be effective. After the dissolving process, HCl was used for neutralization. The final solution contained 50 mM NaCl. To have equal conditions, the solution of AFP obtained by all three methods had the same NaCl concentration.

Ice Nucleating Protein

To simplify the experiments of freezing, by means of reducing the liquid supercooling and therefore achieving more

predictable crystal initiation, an ice nucleating protein released from the ice nucleating bacteria *Pseudomonas Syringae* was included in the AFP solution. A nucleation temperature of −4.8°C could be obtained with a concentration of ice nucleating protein, corresponding to 3×10^7 bacterial cells/ml AFP solution. However, for investigations of controlled crystal growth, only the ice crystal itself was good enough for nucleation.

Low-Temperature Storage Ability of Ice Slurry

To determine the low-temperature storage ability of the ice slurry created from an AFP solution, a differential scanning calorimeter (DSC) was utilized. The sample of the AFP solution was sealed in an aluminum capsule and placed inside a chamber where the sample and a reference material, Al_2O_3, were exposed to the same temperature-controllable environment. A receiver containing methanol, holding a temperature of about −50°C was covering the chamber, while heat was applied to the sample and the reference through direct conduction from a buffer block for obtaining the desired temperature. After the creation of ice, the sample and reference were heated at a constant temperature gradient of 0.1°C/min. The heat input difference between the sample and reference as well as the sample temperature were recorded. In Fig. 3, the typical characteristics of melting are shown. Point a) indicates the start of melting, point b) indicates the melting process is finished, while at point c) the temperature gradient of the sample has returned to its original 0.1°C/min. The total amount of heat involved in the phase change can be found as the area between the curve and a straight line between point a) and point c) (area A and B in Fig. 3). To find the accumulated low-temperature energy as a function of the AFP ice slurry's temperature, it was necessary to recalculate from the obtained values of heat input difference.

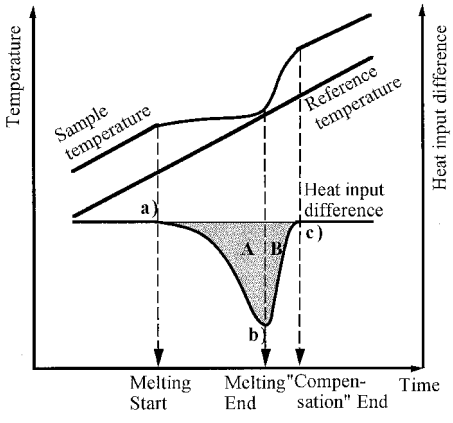

Fig. 3 Measurement characteristics using DSC when melting.

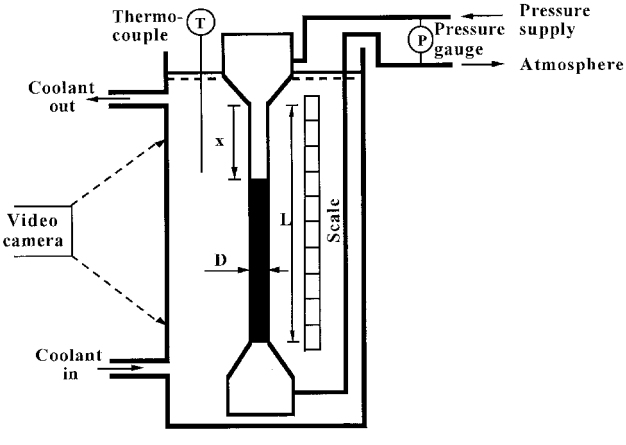

Fig. 4 Capillary tube viscometer used for experiments.

Measurement of Slurry's Effective Viscosity by a Capillary Tube Viscometer

The flowability of ice slurry can be expressed through the viscosity relations or by determining the pressure drop relations during flow. A fluid's viscosity is found by measuring the shear stress and shear rate. Since the amount of the AFP solution available was limited, a capillary tube viscometer made of glass was constructed, similar to an hour glass, for the investigation of the ice slurry viscosity. The principal of this method is to measure the frictional pressure drop in laminar flow for a fluid in a long, smooth cylindrical tube with known dimensions and at a given shear rate.

As shown in Fig. 4, a capillary tube with an i.d. of 2.5 mm and a length of 220 mm was used, giving a length/i.d. ratio large enough to omit end effects.[13] The hour glass was placed in a temperature-controlled ethanol bath. The creation of ice slurry was obtained by freezing the AFP solution inside the tube and then adjusting to the desired temperature over a long period to obtain a uniform condition for slurry in the tube. Effective viscosity μ_e is the viscosity that makes Poiseuille's equation fit any set of laminar flow characteristics for time-independent fluids. It can be found as the derived shear rate/shear stress ratio and can, in principle, be applied to non-Newtonian fluids as well, if the effective viscosity is related to the derived shear rate $8V/D$ (Ref. 13). Including values at different positions in the capillary tube during flow through, the equation becomes

$$\mu_e(x) = \frac{D\Delta P_f(x)/4(L - x)}{8V(x)/D} \tag{1}$$

The velocity was measured by a high-speed camera and the pressure difference recorded both parameters relative to the position x.

Measurement of Ice Slurry Pressure Drop for Flow in a Loop

To examine the ice slurry flow characteristics during tube flow, similar to what would be the situation in real applications, a horizontally arranged loop was constructed as shown in Fig. 5 for measuring the pressure drop. The straight lines were made of glass tubes, whereas the bends were made of an elastic vinyl hose, with all parts being 6.0 mm i.d. The diameter was chosen as large as possible for the limited amount of AFP available. The experimental apparatus was put in a temperature-controlled room, set at the slurry operational temperature (−0.5 to 0°C) to avoid the influence of heat leakage. Furthermore, for slurry temperature adjustments, the glass tubes were covered by a parallel ethanol flow, temperature controlled by a separate ethanol cooler. Slurry temperature was measured using a thermistor and a sensor inserted into the slurry flow; whereas the pressure drop was measured for the 1-m straight glass tube. The flow rate could be controlled by a pump having a maximum speed of 1.0 m/s.

To create the desirable ice slurry condition for the experiments, the following procedure was used: 1) creation of seed

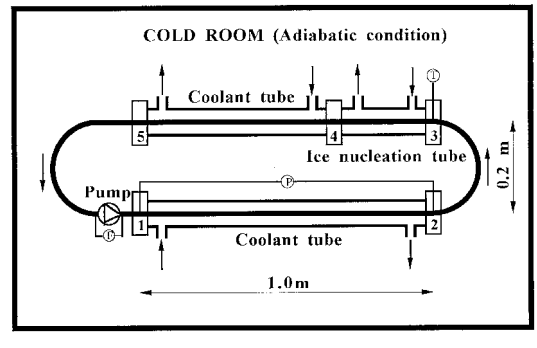

Fig. 5 Ice slurry loop used for experiments.

crystals in heat exchanger 3-4 at the nucleation temperature (decided by the ice nucleation protein), 2) distribution of seed crystals to the whole loop using the pump for a few seconds, 3) melting the dendritic–crystal-based compact ice in heat exchanger 3-4 while growing needle type crystals from seed crystals in heat exchanger 1-2 and 4-5, 4) adjustment of operation temperature in all heat exchangers and starting ice slurry flow, and 5) obtaining steady-state condition and recording flow temperature and pressure difference.

Results and Discussion

Observation of Ice Crystal Structure

An investigation of the dynamic process of ice crystal growth influenced by AFP adsorption has been performed by Coger et al.[12] They reported that an AFP concentration of 1 mg AFP per ml water is high enough to guarantee modifications in the ice crystal structure caused by freeze inhibition. Between 1–10 mg/ml, the spicular or needle-type crystals dominate.

The purpose of observing the ice crystal growth in our research was not only to detect the shape of crystals, but also to see the influence of mechanical disturbance, since this is important for the flowable ice slurry. Experiments were performed in a −5°C room, observing crystals under an optical microscope through polarized plates. Ice crystals were growing from inserted seed ice in an AFP solution exposed only to the surrounding low temperature.

In the experiments using an AFP concentration of 5 mg/ml, the importance of supercooling for ice crystal formation was observed qualitatively. If seed ice crystals were inserted in a highly supercooled solution, dendritic crystals were created instead of the characteristic needle-type ones and the growth occurred at high speed. The formation of such crystals indicates that the potential for growth, caused by the high supercooling, resulted in a growth that is too fast for the AFP to adsorb to the ice crystal surface. At growth-initiating temperatures corresponding to low supercooling, above the critical value for dendritic growth, the typical needle-type crystals could be observed (Fig. 6). Here, the AFPs are successfully adsorbing to the surface and control the growth, occurring parallel to the prism faces. The growth continues as long as there is a thermodynamic potential in the adjacent surroundings of the crystal, corresponding to a temperature just below the local freezing point. The more seed crystals there are in the solution, the higher the number of needle crystals becomes. Mechanical disturbance during this growth will easily cut the needles into smaller pieces, which can act as additional seed crystals. Figure 7 shows a situation after mechanical disturbance. There is no binding between two crystals' prism face surfaces, but they exist separately from each other. Furthermore, when the thermodynamic potential for growth is not present, and when the temperature is lower than the melting point (within the thermal hysteresis gap), the growth of long needle crystals is stopped and at the same time there will be no melting. For ice storage purposes these factors are important, since no mechanical stirring is necessary because of the lack of recrystallization and the slurry can remain unchanged within the temperature range of the hysteresis.

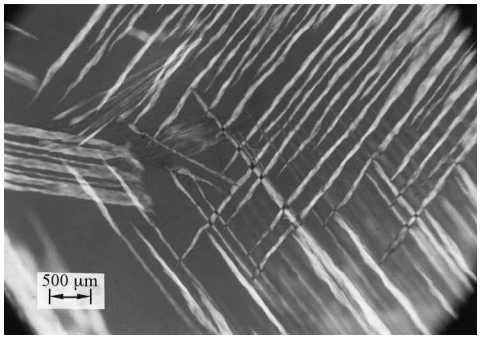

Fig. 6 Characteristic needle-type ice crystals.

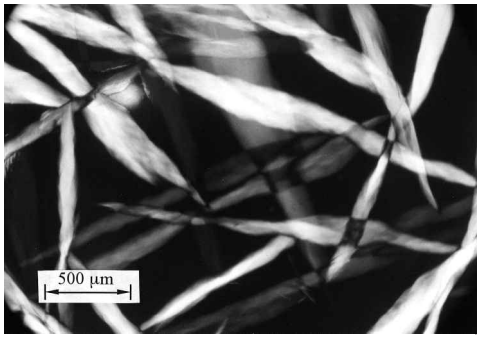

Fig. 7 Needle-type crystals after mechanical disturbance. They exist as individual crystals, not connected to each other.

For the design of heat exchangers utilizing ice slurry made from AFP solutions, the control of heat flux will be important to avoid the supercooling to exceed the critical value for dendritic growth and by that obtain needle-type crystals affected by adsorbed AFPs.

Stored Enthalpy as a Function of Slurry Temperature

In Fig. 8, the results for four different AFP concentrations are shown for the melting case. The values for pure water are also included for comparison. The freezing characteristics will show a different picture because of the effective depression of the freezing point. In Fig. 8, the 6-mg/ml case is shown for comparison with the corresponding melting characteristics. The important information from such a description is the value of the hysteresis gap, where apparently no freezing or melting occurs.

For the melting case, the values from −0.3°C up to the equilibrium melting temperature are quite equal for the four concentrations. However, for values lower than −0.3°C, the influence of the difference in concentration is considerable. −0.3°C represents approximately 100 kJ/kg accumulated heat, corresponding to 30% of the latent heat of pure water. At −1.0°C, the main part of the latent heat is accumulated in ice, corresponding to 285 kJ/kg in the case of 6 mg/ml, which represents 85% of the latent heat of pure water.

Effective Viscosity and Pressure Drop as a Function of Slurry Temperature

In Fig. 9, the effective viscosity for the ice slurry, consisting of 6 mg/ml AFP, is presented as a function of the derived shear rate $8V/D$ for various temperatures. The initial shear stress observed indicates that the ice slurry has a Bingham fluid characteristic. Increasing the temperature seems to have a significant effect on the effective viscosity reduction. In Table 1,

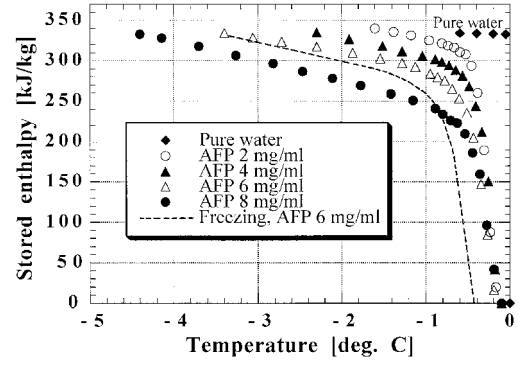

Fig. 8 Stored enthalpy as a function of melting temperature for four AFP concentrations. The freezing characteristics for 6 mg/ml are also indicated.

Table 1 Approximated correlation between the ice slurry temperature (and ice content) and the effective viscosity ratio between ice slurry made from a 6-mg/ml AFP solution and liquid pure water[a]

Slurry temperature, °C	Content of ice, %	Effective viscosity ratio
−0.3	30	2
−0.4	60	100
−0.5	70	250
−0.6	75	500

[a]The −0.3°C case is measured by the slurry loop. Shear rate value is 1000 s^{-1}.

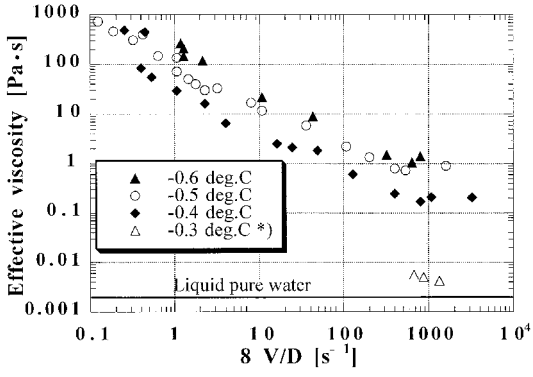

Fig. 9 Effective viscosity as a function of derived shear rate 8*V*/*D*. *), the −0.3°C case is measured by the slurry loop for an AFP concentration of 5 mg/ml.

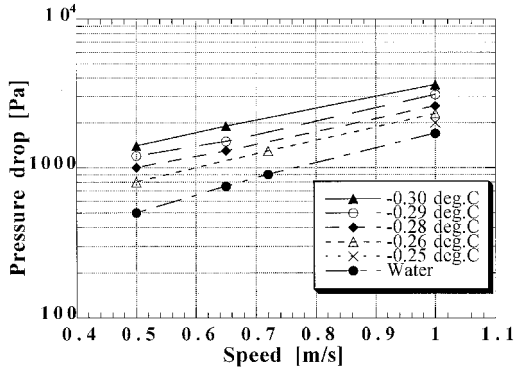

Fig. 10 Pressure drop in the 1.0-m-long horizontal glass tube as a function of flow velocity for various temperatures.

values from Figs. 8 and 9 have been compared. At a temperature of −0.6°C, 250 kJ/kg stored enthalpy is involved. This corresponds to 75% of the latent heat of pure water, which also indicates the content of ice in the slurry.

The steep curve for the melting characteristic in Fig. 8 indicates the strong temperature dependency of stored enthalpy. A small change in temperature in this area will change the content of ice dramatically and the flowability will necessarily be strongly influenced.

In Fig. 10 the pressure drop/speed relation for flow in the loop is shown for various temperatures at an AFP concentration of 5 mg/ml. Also, the liquid pure water case is shown as a reference. Increasing the slurry speed reduces the pressure drop ratio between ice slurry and liquid pure water. In the −0.30°C case, the pressure drop for the ice slurry is around twice at 1 m/s, while in the case of 0.5 m/s, it is around three times. When designing ice storage systems these results are important for finding the suitable operational condition.

If we correlate the pressure drop of the ice slurry to the value for pure water and use this as an indication of slurry

Fig. 11 Photograph showing needle-type crystals in a glass tube growing from the distributed seed crystals.

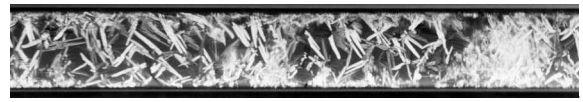

Fig. 12 Photograph showing needle-type crystals in a glass tube after the growth from seeds is completed.

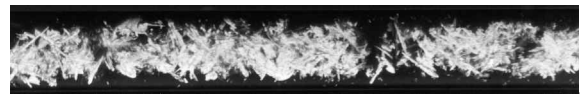

Fig. 13 Photograph showing the typical situation of slurry flow in the loop.

viscosity, we can present the loop results to be compared with the values obtained using the capillary tube viscometer. In Fig. 9, the loop values are included, within the limited range of shear rate, decided by the pump. A significant drop in effective viscosity can be seen for a reduction in ice content from 60 to 30%.

For evaluating ice slurry systems using AFP as the additive, the knowledge about ice crystal shape and size when flowing in tubes is important. In Figs. 11–13, photographs from loop operation are presented. When ice crystals grow from seed particles in a nonflow condition, the characteristic needle-type crystals can be observed (Fig. 11). The whole volume inside the tube, not only the AFP solution at the glass surface heat exchanging area is supercooled within the range of needle crystal growth. Figure 12 shows the situation when the growth is nearly complete (no growth potential). When slurry is flowing, the mechanical disturbances from the pump and the crystal/crystal interaction breaks the long needles into shorter ones. Figure 13 is a typical photograph, showing steady slurry flow. Crystals flow uniformly in the core, while the liquid is effectively lubricating the surface. In the case of 30% ice content, the Bingham characteristic can hardly be seen because of the low value of the initial shear stress. However, as the pressure drop and viscosity figures show, the tendency for increased flowability at higher shear rates is still present. Obtaining microscale knowledge about the growth inhibition mechanisms when AFPs are adsorbing to the ice surface can make it possible to create even more advanced crystal structures, minimizing flow resistance.

For the design of heat exchangers it will be important to control the supercooling to generate the needle-type crystals as well as to ensure the presence of seed ice. Since the ice crystals have resistance to recrystallization, there will be no need for continuous stirring in the storage tank, which will be beneficial for long-term storage.

AFP Molecular Long-Term Stability

One challenge when using AFP for ice storage is the possibility for degradation of the protein during operation and storage. In a nonsterile condition the protein molecule might be damaged because of digestion by bacteria. However, always keeping the AFP solution at a low temperature reduces the bacterial activity and prevents the AFP from damage. To determine any degradation, we compared the HPLC charts before and after utilizing the AFP in the loop experiments. No additional peaks that could indicate any degradation of the AFP could be detected. Furthermore, 50–100 times of repeated freezing and thawing did not influence the ability for growing needle crystal ice.

Table A1 Relative uncertainty estimations in the viscometer experiments for a given velocity

Velocity, m/s	Pressure difference, %	Column height, %	Velocity, %	Diameter, %	Effective viscosity, %	Shear rate, %
3×10^{-5}	±2	±0.3	±0.5	±2	±3.5	±2.1
3×10^{-4}	±2	±0.5	±1	±2	±3.6	±2.2
3×10^{-3}	±2	±1.5	±3	±2	±4.8	±3.6
3×10^{-2}	±2	±3	±6	±2	±7.6	±6.3
3×10^{-1}	±2	±5	±30	±2	±30.6	±30.1

Conclusions

To evaluate ice slurry made from an antifreeze protein solution for low-temperature storage applications, molecularly–biologically synthesized protein has been used, and the stored enthalpy as a function of the temperature as well as the effective viscosity and pressure drop as a function of temperature have been experimentally investigated and the following conclusions made:

1) For AFP concentrations ranging from 2 to 8 mg/ml, needle-type crystals are created when the supercooling is low. Because of the adsorption of AFPs to the surface of ice, the crystals have the ability not to recrystallize, which is important for long-term storage considerations.

2) In the case of an ice slurry containing 30% ice (30% of the latent heat of pure water), the pressure drop of a flow inside a 6 mm tube at a speed of 1 m/s is twice the pressure drop of liquid pure water. The fluid shows a typically Bingham fluid characteristic.

3) At a temperature of −1.0°C, most of the latent heat in the AFP solution is accumulated in ice. Since the content of ice in the slurry is strongly related to the temperature, the control of the temperature of operation is essential to obtain the desirable flowing condition.

4) The feasibility of utilizing ice slurry containing AFP for ice storage applications has been cleared through the investigation of storage ability and flowability.

Appendix: Uncertainty Analysis

Calorimeter Experiments

In the measurements of the ice slurry's stored enthalpy/temperature relation using the differential scanning calorimeter, there are uncertainties involved in the determination of the heat input difference between the reference material and the sample as well as in the temperature (thermocouple). The level of noise for the heat input difference is set to be within 5 μW below 400°C. For the peak value in Fig. 3 this corresponds to 2%. The thermocouple has an accuracy of ±0.05°C. The representation of the ice slurry's stored enthalpy in this report is from the recalculation of the heat input difference to express the dependency of temperature. It is necessary to define the temperature where the sample is considered to be frozen, coming from a negligible change in heat input difference at the lower temperatures in Fig. 3. Furthermore, the recalculation includes an integration equal to the sum of trapezoids of 70 time-steps with an estimated uncertainty of less than 1%. The freezing estimation that is based on three measurement points is given to show the trend for thermal hysteresis.

Viscometer Experiments

For the representation of effective viscosity as a function of the derived shear rate, there are four input parameters involving uncertainty: 1) pressure difference (pressure transducer) for the fluid to pass through the capillary tube, 2) estimation of the slurry column height inside the tube, 3) slurry column velocity (recorded as the time for the column to flow steps of 5 mm), and 4) given inner diameter. In addition there is temperature, recorded by a thermocouple. In Table A1, the values are presented. The relative uncertainty is varying when changing the slurry column height as well as the velocity. At higher velocities the accuracy drops as a result of limitation in the high-speed camera recording. Temperatures are given by an accuracy of ±0.05°C.

Loop Experiments

For the experiments of slurry flowing in a straight tube, there are three measured parameters involved: 1) temperature (by thermistor), 2) pressure drop (by absolute pressure transducer), and 3) volumetric flow (included in the pump by recording the rotation speed). The accuracy of the thermistor is ±0.005°C. The pressure difference coming from the measurement of the absolute pressure at the two points is estimated within ±8%, based on repeatability considerations. Slurry velocity is based on the measured volumetric flow for the given inner tube diameter of 6.0 mm (±0.05 mm) and is given an accuracy of ±0.25%.

Acknowledgment

The authors gratefully acknowledge the collaboration of P. E. Frivik of SINTEF Energy, Norway.

References

[1]Paul, J., "Binary Ice—Technologies for the Production of Pumpable Ice-Slurries," *Proceeding of the Institute of Refrigeration*, Session 1992–1993, Inst. of Refrigeration, London, 1993, pp. 5-1–5-10.

[2]Moriya, M., Tanino, M., Kikuchi, S., Hayashi, T., Okonogi, T., and Kozawa, Y., "An Ice Storage System Using Supercooled Water," *Transactions of the Japanese Association of Refrigeration*, Vol. 12, No. 3, 1995, pp. 253–284.

[3]Watanabe, Y., Yamashita, K., Hachimonji, T., and Noma., T., "Experimental Study on Frazil Ice Formation and Characteristics of Direct Heat Transfer Between Two Liquids," *Proceedings of the 2nd International Conference on Multiphase Flow*, Japan Society of Multiphase Flow, Kyoto, Japan, 1995, EN-25–31.

[4]DeVries, A. L., and Lin, Y., "Structure of a Peptide Antifreeze and Mechanism of Adsorption to Ice," *Biochimica et Biophysica Acta*, Vol. 495, No. 2, 1977, pp. 388–392.

[5]Feeney, R. E., and Burcham, T. S., "Antifreeze Glycoproteins from Polar Fish Blood," *Annual Review of Biophysics and Biophysical Chemistry*, Vol. 15, 1986, pp. 59–78.

[6]Yang, D. S. C., Sax, M., Chakrabartty, A., and Hew, C. L., "Crystal Structure of an Antifreeze Polypeptide and Its Mechanistic Implications," *Nature*, Vol. 333, No. 6170, 1988, pp. 232–237.

[7]Knight, C. A., Cheng, C. C., and DeVries, A. L., "Adsorption of α-Helical Antifreeze Peptides on Specific Ice Crystal Surface Planes," *Biophysical Journal*, Vol. 59, No. 2, 1991, pp. 409–418.

[8]Knight, C. A., Wen, D., and Laursen, R. A., "Nonequilibrium Antifreeze Peptides and the Recrystallization of Ice," *Cryobiology*, Vol. 32, No. 1, 1995, pp. 23–34.

[9]Chakrabartty, A., Ananthanarayanan, V. S., and Hew, C. L., "Structure-Function Relationships in a Winter Flounder Antifreeze Polypeptide," *Journal of Biological Chemistry*, Vol. 264, No. 19, 1989, pp. 11,307–11,312.

[10]Pickett, M., Scott, G., Davies, P., Wang, N., Joshi, S., and Hew, C., "Sequence of an Antifreeze Protein Precursor," *European Journal of Biochemistry*, Vol. 143, No. 1, 1984, pp. 35–38.

[11]Entis, E. Z., "Industrial Applications of Antifreeze Proteins," *Advances in Heat and Mass Transfer in Biological Systems*, American Society of Mechanical Engineers, HTD-Vol. 288, New York, 1994, pp. 55, 56.

[12]Coger, R., Rubinsky, B., and Fletcher, G., "Microscopic Pattern of Ice Crystal Growth in the Presence of Thermal Hysteresis Proteins," *Heat Transfer in Phase Change*, American Society of Mechanical Engineers, HTD-Vol. 205, New York, 1992, pp. 37–46.

[13]Skelland, A. H. P., *Non-Newtonian Flow and Heat Transfer*, Wiley, New York, 1967, pp. 28–39.